Polar modes and overtone states in Raman spectra of lithium tantalate crystals

V. S. Gorelik[1,2] and A. Yu. Pyatyshev[1,*]

[1]*P. N. Lebedev Physical Institute of the Russian Academy of Sciences, Leninskij Prospekt 53, 119991 Moscow, Russia*

[2]*Department of Physics, Faculty of Fundamental Sciences, Bauman Moscow State Technical University, 2nd Baumanskaya Street 5, 105005 Moscow, Russia*

(Received 2 January 2021; revised 13 June 2021; accepted 29 June 2021; published 13 July 2021)

The conditions for the excitation of transverse and longitudinal polar modes in the processes of Raman scattering of light in mono- and polydomain lithium tantalate single crystals are established using a backscattering geometry. The relative intensity of the overtone Raman spectrum on the longitudinal and transverse fundamental polar excitations is much higher in the polydomain sample. Unfortunately, the exact reason for the difference in the Raman spectra of the mono- and polydomain lithium tantalate samples is unknown. The frequencies of the two overtone bands exceeded the exact value of the overtone frequency corresponding to the fundamental longitudinal polar mode $4A_1(\mathrm{LO})$, which clearly indicates the existence of bound phonon pairs (biphonons). This is consistent with theory and has been shown for both mono- and polydomain samples. On the basis of the general theory of bound states of quasiparticles, the possibility of the existence of bound states of quadrupole excitations of the antipolar type in the vibrational spectrum of a polydomain crystal of lithium tantalate is predicted.

DOI: 10.1103/PhysRevB.104.024303

I. INTRODUCTION

Dielectric materials widely used in acoustoelectronics, optoelectronics, and robotics [1–4] include single crystals based on oxide compounds of tantalum, the most important of which is the ferroelectric crystal of lithium tantalate ($LiTaO_3$, LT). At room temperature, this crystal is a pyroelectric and is characterized by a high value of spontaneous polarization (50 $\mu C/cm^2$ [5]). The properties of the $LiTaO_3$ crystal largely depend on the presence of defects that arise during crystal growth or under the influence of external disturbances. Therefore, the study of the optical properties of LT, both pure and with various impurities and defects, is an urgent problem.

The vibrational spectrum of a uniaxial LT crystal contains transverse and longitudinal polar modes, which are allowed by the selection rules for observation in both infrared and Raman spectra due to the absence of an inversion center in the point symmetry group in the pyroelectric phase ($T < T_c$). In the spectra of spontaneous Raman scattering of the first order of LT crystals, Raman lines corresponding to scattering by transverse (TO) and longitudinal (LO) polar modes were found [6–11]. Until recently, studies of LT crystals were limited to the analysis of first-order Raman processes accompanied by the excitation (or relaxation) of single-particle states of polar modes. Reference [12] reported the manifestation of overtone bands in the Raman spectrum of a LT single crystal in the spectral range of 1300–1920 cm^{-1}. In the second-order Raman spectra, previously studied in a number of crystals [13–17], pairs of phonons with oppositely directed quasimomenta corresponding to the boundary or inner region of the Brillouin zone appeared. Previously, the intensity peaks observed in second-order Raman spectra in crystals were interpreted as anomalies in the density of free two-phonon states. The conditions for the manifestation of so-called bound states of pairs of phonons (biphonons) in these spectra were also analyzed.

In this work, the task is to investigate the full Raman spectrum of polar excitations in lithium tantalate crystals in the backscattering geometry in a wide spectral region, including both the range of fundamental polar modes and the region of the second-order Raman spectrum corresponding to the manifestation of pairs of free and coupled polar excitations.

II. DESCRIPTION OF SAMPLES FOR RESEARCH

At room temperature $LiTaO_3$ is in the ferroelectric phase and is a uniaxial optically negative crystal. The space symmetry group C_{3V}^6 ($R3c$) belongs to the rhombohedral system. The unit cell parameters have the following values: $a = 5.15$ Å and $c = 13.78$ Å, with 2 f.u. in a unit cell [18–20]. At a temperature $T_c = 898$ K [21], a ferroelectric phase transition to the paraelectric phase occurs in this crystal. Upon slow cooling of a LT single crystal near T_c, the sample can be brought to a monodomain state by applying a small electric field directed along the optical Z axis. Without an electric field at $T < T_c$, the single crystal decomposes into antiparallel (180°) polarized domains collinear with the Z axis. The space group of the symmetry of the paraelectric phase is D_{3d}^6 ($R\bar{3}c$).

The optical representation specifying the types of symmetries of polar optical modes at $k = 0$ in the pyroelectric phase of LT has the form

$$T_{\mathrm{opt}} = 4A_1(Z) \oplus 9E(X, Y) \oplus 5A_2 \quad (1)$$

*jb_valensia@mail.ru

The structures of the other first- and second-order representations required for analysis are

$$\begin{aligned} V &= A_1(Z) \oplus E(X,Y), \\ [V]^2 &= 2A_1(Z) \oplus 2E(X,Y), \\ [A_1(Z)]^2 &= A_1(Z), \\ [E(X,Y)]^2 &= A_1(Z) \oplus E(X,Y), \\ [A_2]^2 &= A_1(Z). \end{aligned} \tag{2}$$

From relations (1) and (2) it follows that the polar modes $A_1(Z)$ and $E(X,Y)$ are allowed by the selection rules for observation in first-order Raman processes; vibrations of types $A_1(Z)$, $E(X,Y)$, and A_2 are allowed in second-order Raman processes (for overtone transitions).

For this research we used two commercial LT samples in the form of oriented single crystals. Sample 1 is nominally monodomain, cut and polished in the form of a straight prism with dimensions of $10 \times 10 \times 15$ mm^3 with the orientation of the polar Z axis along the largest dimension. Sample 2 has the same dimensions but was subjected to repeated heating and cooling in the region of the ferroelectric phase transformation temperature T_c with a transition to the polydomain state at room temperature.

III. EXPERIMENTAL RESULTS

A schematic diagram of the setup for exciting and recording Raman spectra at room temperature using a backscattering geometry and a BWS465-785H spectrometer was presented earlier [12,17,21]. Spontaneous Raman scattering in the studied crystals was excited by a cw semiconductor laser with a power of up to 100 mW and a radiation wavelength of $\lambda = 785$ nm. The use of exciting infrared radiation ensured the absence of the formation of optical distortions ("optical damage") under the action of intense laser radiation. Exciting laser radiation was introduced into the first channel of a two-channel fiber and focused after leaving the fiber with the help of two lenses onto the surface of the sample under study along or perpendicular to the polar Z axis. The focal waist was at the center of the crystal under study, which ensured a small divergence of the exciting radiation inside the single crystal under study. The scattered light was collected by the same lenses in the opposite direction and was introduced into the second channel of the fiber. After a selective light filter that cuts off the exciting radiation, the Raman signal entered the slit of a BWS465-785H spectrometer with a multielement detector, which allows recording the Raman spectrum in the range of 50–2850 cm^{-1}. In accordance with the fact that we used a backscattering geometry, the wave vector of polar excitations, which appear in the first-order Raman spectra, was comparable to the wave vector of exciting radiation: $k_p \approx 2k_{las} \approx 10^5$ cm^{-1}. We did not use polarizers, and control of the polarization of the scattered radiation was not carried out.

Figures 1(a)–1(d) show the recorded Raman spectra for samples 1 and 2. In this case, two scattering geometries were used: $Z(XX;YY;XY)\underline{Z}$ [Figs. 1(a) and 1(c)] and $X(ZZ;ZY)\underline{X}$

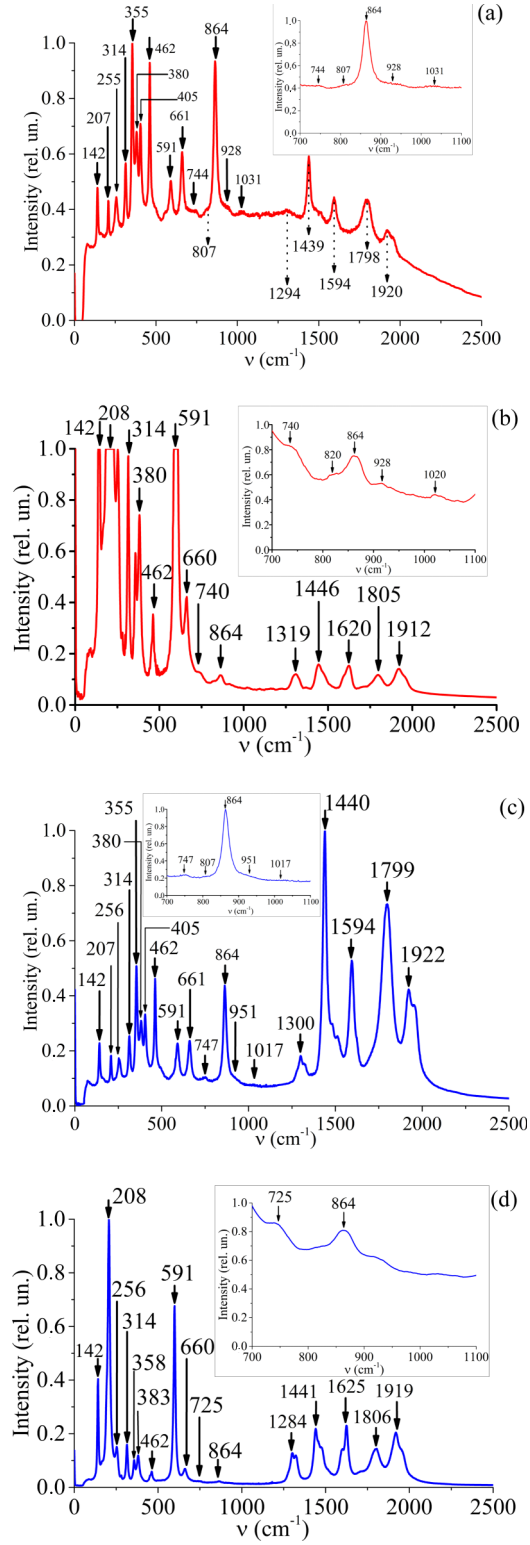

FIG. 1. Raman spectra in the region of fundamental modes and overtone transitions for the backscattering geometry of samples (a) and (b) 1 and (c) and (d) 2 of $LiTaO_3$ with the optical Z axis oriented (a) and (c) along the direction of propagation of the exciting radiation [geometry $Z(XX;YY;XY)\underline{Z}$] and (b) and (d) perpendicular to this direction [geometry $X(ZZ;ZY)\underline{X}$].

TABLE I. Frequencies (in cm^{-1}) of the transverse (TO) and longitudinal (LO) polar modes of $LiTaO_3$, taking into account the data obtained in this work and in [10,21].

No.	$A_1(Z;\mathrm{TO})$	$A_1(Z;\mathrm{LO})$	$E(X,Y;\mathrm{TO})$	$E(X,Y;\mathrm{LO})$
1	207	255	142	190
2	256	355	208	211
3	358	405	256	279
4	661	864	314	349
5			372	380
6			383	453
7			462	472
8			591	660
9			661	864

[Figs. 1(b) and 1(d)]. As seen from Figs. 1(a) and 1(b), the spectrum of sample 1 contains intense Raman lines $1A_1(Z;\mathrm{LO})$, $2A_1(Z;\mathrm{LO})$, $3A_1(Z;\mathrm{LO})$, and $4A_1(Z;\mathrm{LO})$, corresponding to longitudinal polar modes with polarization along the Z axis. In addition, in accordance with the form of the Raman tensor [22,23], doubly degenerate transverse $1E(X,Y;\mathrm{TO})$, $2E(X,Y;\mathrm{TO})$, $3E(X,Y;\mathrm{TO})$, $4E(X,Y;\mathrm{TO})$, $5E(X,Y;\mathrm{TO})$, $6E(X,Y;\mathrm{TO})$, $7E(X,Y;\mathrm{TO})$, $8E(X,Y;\mathrm{TO})$, and $9E(X,Y;\mathrm{TO})$ vibrations are observed for the same geometry. The number in front of the irreducible representation denotes how many such vibrations of the A_1 and E symmetries with different energies are allowed for LT. According to the results of the group-theoretic analysis, one cannot determine the ratio energies of these different vibrations of the same type of symmetry. Table I shows the values of all the frequencies of the main polar modes of the LT crystal measured in this work and known from the literature. As can be seen from Table I, significant differences in frequencies are observed for the TO and LO modes, which is characteristic of polar vibrations in noncentrosymmetric crystals. The strong anisotropy of the LT crystal lattice leads to differences in the vibration frequencies along the (A_1 mode) and perpendicular to (E mode) the polar axis.

In the region of 50–864 cm^{-1} for sample 1, intense Raman peaks corresponding to first-order processes are found. A similar situation in this region of the spectrum is observed for sample 2 [see Figs. 1(c) and 1(d)]. In addition, weak second-order Raman bands are found in the frequency range of 700–1000 cm^{-1}. In particular, the 744–747 cm^{-1} band (see Fig. 1) slightly exceeds the exact value of the overtone frequency (710 cm^{-1}) of the $2A_1(\mathrm{LO})$ mode. A similar situation is realized for weak second-order bands with frequencies 807–820, 928–951, and 1017–1031 cm^{-1}. In the high-frequency region of the Raman spectrum (1100–2200 cm^{-1}), the presence of several intense second-order bands corresponding to overtone processes was found for both samples. This effect is especially pronounced for sample 2 [see Figs. 1(c) and 1(d)]. In this case, the intensity of the overtone bands is comparable to or even exceeds the intensity of the fundamental Raman lines. Unfortunately, the exact reason for the difference in the Raman spectra of the two studied LT samples is unknown.

In the case of longitudinal polar waves, the group velocity weakly depends on the value of the wave vector k and is very small ($V_{gr} \sim 10^2$–10^3 m/s). For transverse polar waves with wave vectors $k \geqslant 10^5$ cm^{-1}, their group velocity is also low. In the region of small values of wave vectors ($k < 10^4$ cm^{-1}), transverse polar modes are characterized by a sharp dependence of the frequency on the wave vector and a significant increase in the group velocity of the corresponding waves, comparable to the speed of light in vacuum.

The theory of the formation of bound states of phonons in crystals was previously developed in [15–17,24–28]. Let us consider the application of a similar theory to describe bound states of polar excitations (biphonons). The model Hamiltonian for two point-interacting quasiparticles is written as

$$\hat{H} = \sum_{\vec{k}} \hbar\omega(\vec{k})[a^{+}_{\vec{k}} a_{\vec{k}}] + \frac{g_4}{4!V}\int \psi(\vec{r},t)\psi(\vec{r},t)\psi(\vec{r},t)\psi(\vec{r},t)d^3\vec{r}\,dt,$$

$$\psi(\vec{r},t) = \frac{1}{\sqrt{V}}\sum_{\vec{k}}\sqrt{\frac{\omega(\vec{k})}{2}}\left[a_{\vec{k}} e^{i[\vec{k}\vec{r}-\omega(\vec{k})t]} + a^{+}_{\vec{k}} e^{-i[\vec{k}\vec{r}-\omega(\vec{k})t]}\right]. \tag{3}$$

Here $\omega(\vec{k})$ is the law of dispersion of single-particle states, the form of which is given below; g_4 is the momentum-independent dimensionless anharmonic coupling constant [24], and V is the volume of the analyzed medium. The one-particle Green's function of phonons is defined as follows:

$$D_1(\vec{r},t;\vec{r'},t') = -iT\langle\psi(\vec{r},t)\psi(\vec{r'},t')\rangle. \tag{4}$$

The Fourier component of the one-particle Green's function has the form [29]

$$D_1(\vec{k},\omega) = \frac{\omega(\vec{k})}{2}\left[\frac{1}{\omega-\omega(\vec{k})+\frac{1}{2}i\Gamma} - \frac{1}{\omega+\omega(\vec{k})-\frac{1}{2}i\Gamma}\right]. \tag{5}$$

Two-particle states are described by the Green's function

$$D_2(\vec{r},t;\vec{r'},t') = -iT\langle\psi(\vec{r},t)\psi(\vec{r},t)\psi(\vec{r'},t')\psi(\vec{r'},t')\rangle. \tag{6}$$

The corresponding Bethe-Salpeter equation for the two-particle Green's function is written as a sum of diagrams. The solution to this equation for the coupling of two quasiparticles with the same frequencies and quasimomenta has the form

$$D_2(\vec{r},t;\vec{r'},t') = i[D_1(\vec{r},t;\vec{r'},t')]^2 + ig_4\int[D_1(\vec{r},t;\vec{r_1},t_1) \times D_1(\vec{r_1},t_1;\vec{r'},t')]^2 d\vec{r}\,dt + \cdots, \tag{7}$$

$$D_2(\vec{K}=2\vec{k},\omega) = \frac{2F(\omega)}{1-\frac{1}{2}g_4F(\omega)},$$

$$F(\omega) = \frac{i}{(2\pi)^4}\int d^3\vec{k}\int D_1(\vec{k},\omega-\omega')D_1(-\vec{k},\omega')d\omega'. \tag{8}$$

The density of single-particle states is found from the well-known relationship [30,31]

$$\rho_1(\omega) = \frac{V}{(2\pi)^3}\int \frac{dS_{\vec{k}}}{|\nabla_{\vec{k}}\omega|} = \frac{Vk^2}{2\pi^2}|\frac{dk}{d\omega}|. \tag{9}$$

In the region of small $|\vec{k}|$ near the center of the Brillouin zone the dispersion law is linear for all crystallographic directions, and the dispersion relation is isotropic. Consider longitudinal phonons with a negative effective rest mass. In the quasi-Newtonian approximation of the dispersion law of phonons (as heavy quasiparticles with a negative effective rest mass), the following holds:

$$\omega = \omega_0 - \frac{s^2k^2}{2\omega_0},$$
$$\frac{d\omega}{dk} = -\frac{s^2k}{\omega_0}, \quad \frac{dk}{d\omega} = -\frac{\omega_0}{s^2k},$$
$$\rho_1(\omega) = \frac{Vk^2}{2\pi^2}|\frac{dk}{d\omega}| = \frac{V\omega_0}{2\pi^2 s^3}\sqrt{2\omega_0(\omega_0-\omega)}. \tag{10}$$

We represent the expression for the density of single-particle states in the form

$$\rho_1(\omega) = \alpha\sqrt{\omega_0-\omega}, \quad \alpha = \frac{V\omega_0\sqrt{2\omega_0}}{2\pi^2 s^3}. \tag{11}$$

As a result, for the function $F(\omega)$ we obtain

$$F(\omega) = \frac{1}{4}\omega_0^2\alpha\int_0^{\Delta}\frac{\sqrt{\omega'}}{\omega - 2(\omega_0-\omega') + i\Gamma}d\omega', \tag{12}$$

where Δ is the phonon frequency range taken into account in integration. It is important to note that the function $F(\omega)$ depends on the effective rest mass of the quasiparticle $m_0 = -\frac{\hbar\omega_0}{s^2}$ and on the damping constant Γ associated with the inverse quasiparticle lifetime $\tau = 1/\Gamma$.

For a two-particle density of states proportional to the spectral intensity of the scattered light, taking into account (8), we obtain

$$\rho_2(\omega) = -\frac{1}{\pi\omega_0^2}\mathrm{Im}D_2(\vec{K},\omega)$$
$$\approx -\frac{2}{\pi\omega_0^2}\frac{ImF(\omega)}{\left[1-\frac{1}{2}g_4\mathrm{Re}F(\omega)\right]^2 + \left[\frac{1}{2}g_4\mathrm{Im}F(\omega)\right]^2}. \tag{13}$$

Thus, the calculation of the normalized spectral intensity of the secondary radiation $I(\omega) = \mathrm{Im}D_2(\vec{K},\omega)$ is found using the form of the functions $\mathrm{Im}F(\omega)$ and $\mathrm{Re}F(\omega)$:

$$\mathrm{Im}F(\omega) = \frac{1}{4}\omega_0^2\alpha\int_0^{\Delta}\frac{-\Gamma\sqrt{\omega'}}{[\omega-2(\omega_0-\omega')]^2+\Gamma^2}d\omega',$$
$$\mathrm{Re}F(\omega) = \frac{1}{4}\omega_0^2\alpha\int_0^{\Delta}\frac{[\omega-2(\omega_0-\omega')]\sqrt{\omega'}}{[\omega-2(\omega_0-\omega')]^2+\Gamma^2}d\omega'. \tag{14}$$

The normalized intensity of the bound state in the spectrum of secondary radiation has the form

$$I(\omega) = \frac{2\mathrm{Im}F(\omega)}{\left[1-\frac{1}{2}g_4\mathrm{Re}F(\omega)\right]^2 + \left[\frac{1}{2}g_4\mathrm{Im}F(\omega)\right]^2}. \tag{15}$$

As a result of integration (14), we obtain

$$\mathrm{Im}F(\omega) = \frac{\omega_0^2\alpha}{32\Gamma\psi}\left\{\psi\varphi(\lambda+\omega-2\omega_0)\ln\frac{2\sqrt{\Delta}(\sqrt{\Delta}+\varphi)+\lambda}{2\sqrt{\Delta}(\sqrt{\Delta}-\varphi)+\lambda} + 2\Gamma^2\left[\mathrm{arctg}\left(\frac{\varphi-2\sqrt{\Delta}}{\psi}\right) - \mathrm{arctg}\left(\frac{\varphi+2\sqrt{\Delta}}{\psi}\right)\right]\right\}$$
$$\mathrm{Re}F(\omega) = -\frac{\omega_0^2\alpha}{32\psi}\left\{-8\psi\sqrt{\Delta} + \varphi\psi\ln\frac{2\sqrt{\Delta}(\sqrt{\Delta}-\varphi)+\lambda}{2\sqrt{\Delta}(\sqrt{\Delta}+\varphi)+\lambda} + 2(\lambda+\omega-2\omega_0)\left[\mathrm{arctg}\left(\frac{\varphi+2\sqrt{\Delta}}{\psi}\right) - \mathrm{arctg}\left(\frac{\varphi-2\sqrt{\Delta}}{\psi}\right)\right]\right\},$$

where $\lambda = \sqrt{(\omega-2\omega_0)^2+\Gamma^2}$, $\psi = \sqrt{\lambda+\omega-2\omega_0}$, and $\varphi = \sqrt{\lambda-\omega+2\omega_0}$.

In the quasi-Newtonian approximation of the dispersion law for phonons with a positive effective rest mass, the following holds:

$$\omega = \omega_0 + \frac{s^2k^2}{2\omega_0},$$
$$\frac{d\omega}{dk} = \frac{s^2k}{\omega_0}, \quad \frac{dk}{d\omega} = \frac{\omega_0}{s^2k},$$
$$\rho_1(\omega) = \frac{Vk^2}{2\pi^2}\left|\frac{dk}{d\omega}\right| = \frac{V\omega_0}{2\pi^2 s^3}\sqrt{2\omega_0(\omega-\omega_0)}. \tag{16}$$

In this case, the expression for the density of one-particle states is

$$\rho_1(\omega) = \alpha\sqrt{\omega-\omega_0}, \quad \alpha = \frac{V\omega_0\sqrt{2\omega_0}}{2\pi^2 s^3}. \tag{17}$$

As a result, for the function $F(\omega)$ we obtain

$$F(\omega) = \frac{1}{4}\omega_0^2\alpha \int_0^{\Delta} \frac{\sqrt{\omega'}}{\omega - 2(\omega_0 + \omega') + i\Gamma} d\omega'. \tag{18}$$

And finally, after integrating (18) we get

$$\mathrm{Im}F(\omega) = \frac{\omega_0^2\alpha}{32\Gamma\varphi}\left\{\varphi\psi(\lambda - \omega + 2\omega_0)\ln\frac{2\sqrt{\Delta}(\sqrt{\Delta}+\psi)+\lambda}{2\sqrt{\Delta}(\sqrt{\Delta}-\psi)+\lambda} + 2\Gamma^2\left[\mathrm{arctg}\left(\frac{\psi - 2\sqrt{\Delta}}{\varphi}\right) - \mathrm{arctg}\left(\frac{\psi+2\sqrt{\Delta}}{\varphi}\right)\right]\right\},$$

$$\mathrm{Re}F(\omega) = \frac{\omega_0^2\alpha}{32\varphi}\left\{-8\varphi\sqrt{\Delta} + \varphi\psi\ln\frac{2\sqrt{\Delta}(\sqrt{\Delta}+\psi)+\lambda}{2\sqrt{\Delta}(\sqrt{\Delta}-\psi)+\lambda} + 2(\lambda - \omega + 2\omega_0)\left[\mathrm{arctg}\left(\frac{\psi + 2\sqrt{\Delta}}{\varphi}\right) - \mathrm{arctg}\left(\frac{\psi - 2\sqrt{\Delta}}{\varphi}\right)\right]\right\}.$$

The approximate value of the anharmonicity constant g_4 can be estimated based on the expression $g_4' = \lambda g_4$, where $\lambda = \frac{1}{8}\alpha\omega_0^2\sqrt{\Delta}$ [24]. In the limit $g_4' = 0$ we have the spectral density of two noninteracting phonons in the form $\rho_2(\omega) \approx -\frac{2}{\pi\omega_0^2}\mathrm{Im}F(\omega)$ and have the root dependence on frequency in the region of the exact value of the overtone frequency, which corresponds to the formation of a pair of free phonons in elementary second-order Raman processes. For finite values of g_4', a sharp peak appears, split off from the band of free two-particle states. With a decrease in the value of anharmonicity $g_4' \to 0$, the peak superimposed on the continuous spectrum shifts towards a decrease in energy and broadens significantly. If the anharmonicity is large enough ($g_4' > 1$), the two-phonon bound state splits off from the top of the two-phonon continuum, and a sharp peak appears at energies exceeding twice the maximum one-phonon energy, in accordance with the results [32].

Consider, for definiteness, the overtone state of the longitudinal mode $4A_1(Z;\mathrm{LO})$ with frequency $\nu_0 = 864\ \mathrm{cm}^{-1}$. For the LT crystals under study with dimensions $10 \times 10 \times 15\ \mathrm{mm}^3$, the volume will be $V = 1.5 \times 10^{-6}\ \mathrm{m}^3$; frequency $\omega_0 = 2\pi c\nu_0 = 1.63 \times 10^{14}$ rad/s. Figure 2 shows the results of comparing the calculations of the spectral distribution of Raman scattering in the overtone region $2\nu_0 = 1728\ \mathrm{cm}^{-1}$ and the experimentally observed distribution of the Raman intensity.

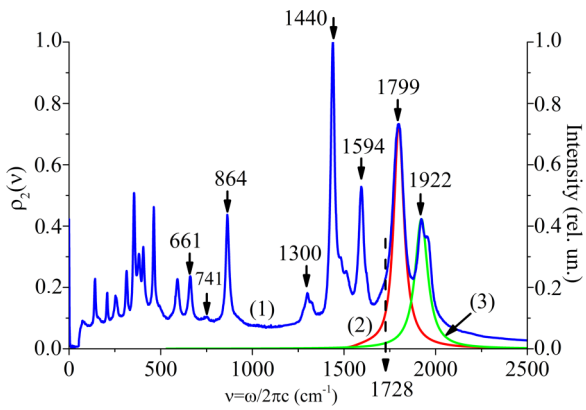

FIG. 2. Comparison of the spectral intensity of Raman scattering for the geometry $X(ZZ;ZY)\underline{X}$ in a polydomain LT single crystal (curve 1) with the calculation in the region of the overtone mode $2\nu_0 = 1728\ \mathrm{cm}^{-1}$ with the calculated curves 2 and 3 for $\rho_2(\nu)$.

As can be seen from Fig. 2, for the band in the region of $1799\ \mathrm{cm}^{-1}$ (curve 2 in Fig. 2), satisfactory agreement for the bound state of the longitudinal polar mode $4A_1(Z;\mathrm{LO})$ with $\nu_0 = 864\ \mathrm{cm}^{-1}$ is achieved at the values $\Delta = 0.1\omega_0$, $s = 1000$ m/s, $\Gamma = 2\pi c \times 40 = 7.53 \times 10^{12}$ rad/s, and $g_4 = 8.52 \times 10^{-40}$. The highest frequency band at $1922\ \mathrm{cm}^{-1}$ (curve 3 in Fig. 2) is interpreted as the overtone of an $4A_1(Z;\mathrm{LO})$-type phonon ($\nu_0 = 864\ \mathrm{cm}^{-1}$) with a positive effective rest mass [Eqs. (16) and (18)]. Satisfactory agreement is achieved at $\Delta = 0.1\omega_0$, $s = 1000$ m/s, $\Gamma = 2\pi c \times 40 = 7.53 \times 10^{12}$ rad/s, and $g_4 = 3.99 \times 10^{-40}$. The region of integration Δ was chosen due to the fact that we are considering a small section of the parabolic dispersion law for phonons near the top of the phonon band. As a constant s, we use a value close to the speed of sound in LT crystal.

The peak at about $1300\ \mathrm{cm}^{-1}$ corresponds to the overtone of the $4A_1(Z;\mathrm{TO})$ mode ($\nu = 661\ \mathrm{cm}^{-1}$); an intense maximum with a frequency of $1440\ \mathrm{cm}^{-1}$ corresponds to the overtone of the $9E(\mathrm{TO})$ mode ($\nu = 741\ \mathrm{cm}^{-1}$). The maximum in the spectrum with a frequency of $1594\ \mathrm{cm}^{-1}$ can be associated with the overtone of phonons with an anomalously low group velocity in the region of $797\ \mathrm{cm}^{-1}$.

IV. CONCLUSION

In a polydomain lithium tantalate single crystal, anomalously intense Raman peaks were found in the overtone region of polar fundamental vibrations. In this case, two bands were found whose frequencies (1799 and $1922\ \mathrm{cm}^{-1}$) exceeded the exact value of the overtone ($864 \times 2 = 1728\ \mathrm{cm}^{-1}$) of the $4A_1(Z;\mathrm{LO})$ mode. As a result of a theoretical analysis of the conditions for the formation of a bound state of two polar excitations of the crystal, it was shown that in this case there is a bounding of two longitudinal polar excitations with a frequency of $864\ \mathrm{cm}^{-1}$ with a splitting up from the band of two-particle states at a binding energy of $71\ \mathrm{cm}^{-1}$. The second high-frequency overtone ($1922\ \mathrm{cm}^{-1}$) is interpreted as a coupling of two transverse polar excitations in the vicinity of the $4A_1(Z;\mathrm{LO})$ mode. Bounding of two transverse polar excitations with oppositely directed polarization vectors, i.e., excitation of the quadrupole (antipolar) type, leads to its transformation at the exit from the crystal into vacuum quadrupole electromagnetic excitations [33–37] with antiparallel directions of the vectors of the electric field strength.

The intensity of radiation of such quadrupole electromagnetic excitations in spontaneous Raman scattering, taking into account the intensity of the observed overtone lines and the ratio of the energy of the photons of the exciting radiation to the energy of the biphonon, is approximately 10^{-8} of the intensity of the exciting radiation, i.e., 10^{-10}–10^{-11} W. In the future, it will be of interest to study stimulated Raman scattering by bounded antipolar quadrupole modes, in which the efficiency of excitation of the Stokes components is 1%–10%.

ACKNOWLEDGMENTS

This work was partially supported by RFBR and BRFBR (Grant No. 20-52-04001 Bel_mol_a).

[1] J. Imbrock, S. Wevering, K. Buse, and E. Krätzig, J. Opt. Soc. Am. B **16**, 1392 (1999).
[2] T. Hatanaka, K. Nakamura, T. Taniuchi, H. Ito, Y. Furukawa, and K. Kitamura, Opt. Lett. **25**, 651 (2000).
[3] Y. Xu, *Ferroelectric Materials and Their Applications* (Elseiver, New York, 1991).
[4] Irzaman, R. Siskandar, N. Nabilah, Aminullah, B. Yuliarto, K. A. Haman, and A. Husin, Ferroelectrics **524**, 44 (2018).
[5] K. M. Rabe, C. H. Ahn, and J. M. Triscone (Eds.), *Physics of Ferroelectrics: A Modern Perspective*, Topics in Applied Physics (Springer, Berlin, Heidelberg, 2007).
[6] W. D. Johnston and J. P. Kaminov, Phys. Rev. **168**, 1045 (1968).
[7] C. Raptis, Phys. Rev. B **38**, 10007 (1988).
[8] A. G. Kuznetsov, V. K. Malinovsky, and N. V. Surovtsev, Phys. Solid State **48**, 2317 (2006).
[9] A. Hushur, S. Gvasaliya, B. Roessli, S. Lushnikov, and S. Kojima, Phys. Rev. B **76**, 064104 (2007).
[10] S. Margueron, A. Bartasyte, A. M. Glazer, E. Simon, J. Hlinka, I. Gregora, and J. Gleize, J. Appl. Phys. **111**, 104105 (2012).
[11] V. S. Gorelik and A. Y. Pyatyshev, Phys. Wave Phenom. **28**, 241 (2020).
[12] S. D. Abdurakhmonov and V. S. Gorelik, Opt. Spectrosc. **127**, 587 (2019).
[13] V. S. Gorelik, O. P. Maximov, G. G. Mitin, M. M. Sushchinsky, and P. N. Lebedev, Solid State Commun. **21**, 615 (1977).
[14] M. M. Sushchinsky, V. S. Gorelik, and O. P. Maximov, J. Raman Spectrosc. **7**, 26 (1978).
[15] A. A. Anik'ev, V. S. Gorelik, and B. S. Umarov, Sov. Phys. Solid State **26**, 1679 (1984).
[16] A. A. Anik'ev, B. S. Umarov, and J. F. Scott, J. Raman Spectrosc. **16**, 315 (1985).
[17] V. S. Gorelik and A. Y. Pyatyshev, Diamond Relat. Mater. **110**, 108104 (2020).
[18] S. C. Abrahams and J. L. Bernstein, J. Phys. Chem. Solids **28**, 1685 (1967).
[19] Y. Yamada, N. Niizeki, and H. Toyoda, Jpn. J. Appl. Phys. **7**, 298B (1968).
[20] S. Huband, D. S. Keeble, N. Zhang, A. M. Glazer, A. Bartasyte, and P. A. Thomas, J. Appl. Phys. **121**, 024102 (2017).
[21] V. S. Gorelik, S. D. Abdurakhmonov, N. V. Sidorov, and M. N. Palatnikov, Inorg. Mater. **55**, 524 (2019).
[22] M. S. Dresselhaus, G. Dresselhaus, and A. Jorio, *Group Theory: Application to the Physics of Condensed Matter* (Springer, Berlin, Heidelberg, 2008).
[23] D. L. Rousseau, R. P. Bauman, and S. P. S. Porto, J. Raman Spectrosc. **10**, 253 (1981).
[24] J. Ruvalds and A. Zawadowski, Phys. Rev. B **2**, 1172 (1970).
[25] A. Zawadowski and J. Ruvalds, Phys. Rev. Lett. **24**, 1111 (1970).
[26] A. A. Anik'ev, V. S. Gorelik, and B. S. Umarov, Sov. Phys. Lebedev Inst. Rep. **10**, 41 (1982).
[27] A. A. Anik'ev, V. S. Gorelik, and B. S. Umarov, Sov. Phys. Lebedev Inst. Rep. **11**, 12 (1982).
[28] A. A. Anik'ev and D. E. Edgorbekov, Phys. Solid State **41**, 116 (1999).
[29] A. A. Abrikosov, L. P. Gorkov, and I. E. Dzyaloshinski, *Methods of Quantum Field Theory in Statistical Physics* (Prentice-Hall, Englewood Cliffs, NJ, 1963).
[30] J. C. Phillips, Phys. Rev. **104**, 1263 (1956).
[31] A. A. Maradudin, E. W. Montroll, and G. H. Weiss, *Theory of Lattice Dynamics in the Harmonic Approximation* (Academic, New York, 1963).
[32] M. H. Cohen and J. Ruvalds, Phys. Rev. Lett. **23**, 1378 (1969).
[33] L. B. Okun', Zh. Eksp. Teor. Fiz. **83**, 892 (1982) [Sov. Phys. JETP **56**, 502 (1982)].
[34] V. S. Gorelik, M. A. Dresvyannikov, L. N. Zherikhina, and A. M. Tskhovrebov, Bull. Lebedev Phys. Inst. **41**, 18 (2014).
[35] S. Hoffmann, Phys. Lett. B **193**, 117 (1986).
[36] K. Van Bibber, N. R. Dagdeviren, S. E. Koonin, A. K. Kerman, and H. N. Nelson, Phys. Rev. Lett. **59**, 759 (1987).
[37] J. Jaeckel, J. Redondo, and A. Ringwald, Europhys. Lett. **87**, 10010 (2009).